A Salt-Induced Kinetic Intermediate Is on a New Parallel Pathway of Lysozyme Folding[†]

Oliver Bieri, Gudrun Wildegger, Annett Bachmann, Clemens Wagner, and Thomas Kiefhaber*

Biozentrum der Universität Basel Abteilung Biophysikalische Chemie Klingelbergstr, 70 CH-4056 Basel, Switzerland

Received April 28, 1999; Revised Manuscript Received July 22, 1999

ABSTRACT: Lysozyme folds through two competing pathways. A fast pathway leads directly from a collapsed state to the native protein, whereas folding on a slow pathway proceeds through a partially folded intermediate (I_1). At NaCl concentrations above 100 mM, a second transient intermediate (I_2) is induced as judged by the appearance of an additional apparent rate constant in the refolding kinetics. Monitoring the time course of native molecules and of both intermediates shows that the NaCl-induced state (I_2) is located on neither of the two folding pathways observed at low-salt concentrations. These results suggest that I_2 is a metastable high-energy intermediate at low-ionic strength and is located on a third folding pathway. The folding landscape of lysozyme seems to be complex with several high-energy intermediates located on parallel folding routes. However, the experiments show no evidence for partially folded states on the fast direct pathway.

The characterization of transition barriers separating the ensemble of unfolded polypeptide chains from the native state is an important step toward the understanding of the mechanism of protein folding. For many proteins, partially folded intermediates transiently accumulate during the folding process. These intermediates guide the folding polypeptide along efficient folding pathways (*1*), according to the framework model. Other models proposed that intermediates represent nonproductive local minima on the energy landscape (*2*−*4*). This view seems to be supported by the experimental observation that many small proteins fold rapidly and in a two-state reaction, which suggests that barrier crossing is a single-step process (*5*−*11*). Recently, however, both experimental (*12*−*14*) and theoretical work (*15*, *16*) indicated that transition barriers for fast-folding proteins might be rough, including distinct local minima that represent metastable high-energy intermediates.

Lysozyme from hen egg-white is a well-suited model system to elucidate the role of intermediates for the folding process. A very rapid reaction occurs in the dead-time of stopped-flow mixing during refolding of lysozyme with disulfide bonds intact (*17*−*19*), leading to a collapsed globular state (C), with solvent exposed hydrophobic residues (*20*). The subsequent formation of native protein (N) occurs in two kinetic reactions with relaxation times ($\tau = 1/k_{app}$)[1] of 30 ms and 400 ms at pH 5.2, 20 °C (*21*). The fast formation of native lysozyme represents a direct folding pathway to the native state, whereas the slow formation of native molecules occurs via an folding intermediate (I_1) with a native-like helical structure (*19*) and a native-like size and shape (*20*). The pathways branch at the stage of the rapidly formed collapsed state (ref *22*, Scheme 1).

Scheme 1

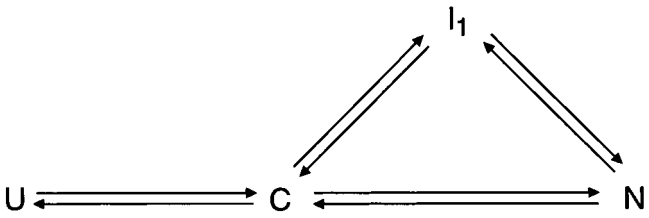

Because of kinetic coupling between the different reactions, the formation of the intermediate and of native molecules on the fast pathway both occur in the faster reaction ($\tau = 30$ ms), whereas the slower reaction represents mainly the interconversion of the intermediate to the native state (*22*). An additional intermediate was shown to be located between collapsed lysozyme and the helical intermediate (*23*). However, this intermediate is higher in energy than the collapsed state and it is thus not observed in refolding reactions.

Although intermediates have been detected and characterized on the slow pathway of lysozyme folding, little is known about the direct-folding reaction. Recently, Kulkarni et al. (*24*) suggested that a native-like state with the α- and β-domains protected from hydrogen exchange is observed on both the fast- and the slow-folding pathway at high-ionic strength. Consequently, formation of this native-like intermediate would represents an essential step in the folding of all lysozyme molecules. Their model was based on the observation of different rate constants for folding monitored by protection from hydrogen exchange and by changes in intrinsic tryptophan fluorescence (*24*). A similar effect has been observed for a lysozyme folding at low-ionic strength and was argued as evidence of an intermediate located on

[†] This work was supported by a grant from the Schweizerischen Nationalfonds (31−46843.96).

* To whom correspondence should be addressed: Phone: ++41-61-267 2194. Fax: ++41−61−267 2189. E-mail: kiefhaber@ubaclu.unibas.ch.

[1] Abbreviations. λ_i: apparent rate constants ($= k_{app}$); k_i: microscopic rate constants; τ_i: time constants ($1/\lambda_i$).

10.1021/bi9909703 CCC: $18.00
Published on Web 08/31/1999

the direct folding pathway (*25*). This model is, however, in contrast to results from interrupted refolding experiments at low-ionic strength, which measure the population of native molecules and of partially folded states. These experiments detected only native lysozyme and the helical intermediate and give the same time constants for formation of the various species as the fluorescence measurements (*21*, *22*).

To investigate the influence of ionic strength on the mechanism of lysozyme folding, we monitored the folding in the presence of NaCl to investigate the resulting effect on the folding kinetics. NaCl was chosen since it is a neutral salt in the Hofmeister series (*26*, *27*), and thus, it should have little effect on protein stability (*28*, *29*). This facilitates comparison of the results with the previously reported data at lower ionic strength (*21*, *22*). Our results show that a third resolvable kinetic reaction is detected by monitoring changes in intrinsic tryptophan fluorescence above 100 mM NaCl, supporting the presence of an additional intermediate (I_2).[2] Monitoring the time course of native molecules and of both intermediates shows that the NaCl-induced state (I_2) is located neither on the direct-folding pathway nor on the slow-folding pathway observed at low concentrations of NaCl. A direct-fast-folding pathway to the native state without detectable intermediates still exists. The results indicate that I_2 is located on a third parallel folding pathway. At a low-ionic strength, I_2 represents a high energy intermediate and thus does not become populated. These results suggest that the energy landscape for lysozyme folding contains several local minima, some of which are only slightly less stable than the unfolded state and may be populated already under only mildly stabilizing folding conditions.

MATERIAL AND METHODS

Materials. Lysozyme (3x crystallized) was purchased from Sigma and was used without further purification. Ultrapure GdmCl (AAA grade) was from Nigu (Waldkraiburg, Germany). All other chemicals were reagent grade and were purchased from Merck (Darmstadt, Germany).

Kinetic Measurements. Direct refolding and unfolding kinetics were monitored by the change in intrinsic tryptophan fluorescence after excitation at 280 nm. Rapid kinetics ($\tau <$ 10 s) were measured in an Applied Photophysics SX18-MV stopped flow instrument by monitoring the change in fluorescence above 320 nm. Typically, 4−10 time traces were averaged. Slow kinetics were measured by manual mixing in an Aminco Bowman SLM Fluorimeter by monitoring the change in fluorescence at 350 nm. The protein concentration was 3.6 μM in both cases. A change in the protein concentration did not affect any of the observed rate constants up to 0.7 mM, which was the highest concentration tested. The presence of mixing artifacts was tested in both instruments by the use of a mixture of *N*-acetyl tryptophanamide and *N*-acetyl tyrosine-amide at the same molar concentration as in lysozyme.

Interrupted Refolding Experiments. Interrupted refolding experiments were performed at 20 °C and at 10 °C to monitor the time course of formation of native molecules or of the folding intermediates. Unfolded lysozyme (in 3.6 M GdmCl, 20 mM glycine/HCl, pH 1.5) was diluted 6-fold into final conditions of 0.6 M GdmCl, 0.85 M NaCl, 50 mM NaOAc, and pH 5.2, which initiated the refolding reaction. After various times (t_i), refolding was interrupted by a second 6-fold mixing step into unfolding conditions of 6.7 M GdmCl, 20 mM Gly, and pH 1.5. Under these conditions, native lysozyme unfolds with a relaxation time of 8 s at 20 °C and of 25 s at 10 °C. Unfolding of the intermediates is complete within 100 ms. The amplitude of the slow unfolding reactions was used as a measure for the amount of native lysozyme present after t_i. The amplitudes were normalized using the unfolding amplitude of the completely refolded solution at $t = \infty$, which was set to 1. The relative amount of folding intermediates generated in the refolding pulse was measured by the same interrupted refolding experiments with unfolding conditions of 5.0 M GdmCl, 0.85 M NaCl, 20 mM NaOAc, and pH 5.2. Under these conditions, the two intermediates unfold with relaxation times of 25 ms and 65 ms at 20 °C and of 50 ms and 200 ms at 10 °C, and native lysozyme unfolds with a relaxation time of 2000 seconds at 20 °C and of 10 000 s at 10 °C; this allows the separation of these processes. The GdmCl-dependence of the two faster rate constants (λ_2 and λ_3) was measured in essentially the same way by applying a refolding pulse of 100 ms and subsequently unfolding the intermediates in the presence of various concentrations of GdmCl.

Equilibrium Transition Curves. The GdmCl-dependence of lysozyme stability was measured by the change in circular dichroism at 225 nm in an Aviv 62 DS spectropolarimeter. The samples were incubated for 12 h at 20 °C or for 24 h at 10 °C to allow for equilibration. The two-state character of the transitions was checked by monitoring the transitions by the change in CD in the aromatic region at 289 nm, which gave identical values as the transition monitored at 225 nm. Protein concentrations were 10 μM in far-UV−CD measurements and 100 μM in near-UV−CD measurements. The path length was 1 cm in both cases.

Data Fitting. Direct refolding and unfolding measurements were fit using the program KinFit (Olis, Bogert, GA) for linear time scales and the program ProFit or the software supplied with the Applied Photophysics stopped-flow instruments for logarithmic time scales. The time course of native molecules and of the folding intermediates were fit simultaneously to the various four-state models displayed in Scheme 2 using the program Scientist (Micromath, Salt Lake City, Utah), which performs nonlinear least-squares fits of the differential equations for the various kinetic mechanisms. To reduce the number of free parameters, we set all unfolding reactions starting from the native state to zero. This approximation is valid, since unfolding of native lysozyme is at least 10^6 times slower than the slowest refolding reaction under the refolding conditions of 0.6 M GdmCl and pH 5.2 (cf. Figures 2A and 4A).

RESULTS

Effect of NaCl on Lysozyme Folding and Stability. We studied the effect of NaCl on the folding mechanism of lysozyme. Refolding kinetics at pH 5.2, 0.6 M GdmCl at 20 °C can be described by the sum of two exponentials with time constants ($\tau = 1/k_{app} = 1/\lambda$) of 33 ± 2 ms and of 385

[2] The two intermediates observed at high-ionic strength are named I_1 and I_2, with I_1 corresponding to the intermediate, which is also observed at low-ionic strength and I_2 corresponding to the salt-induced intermediate.

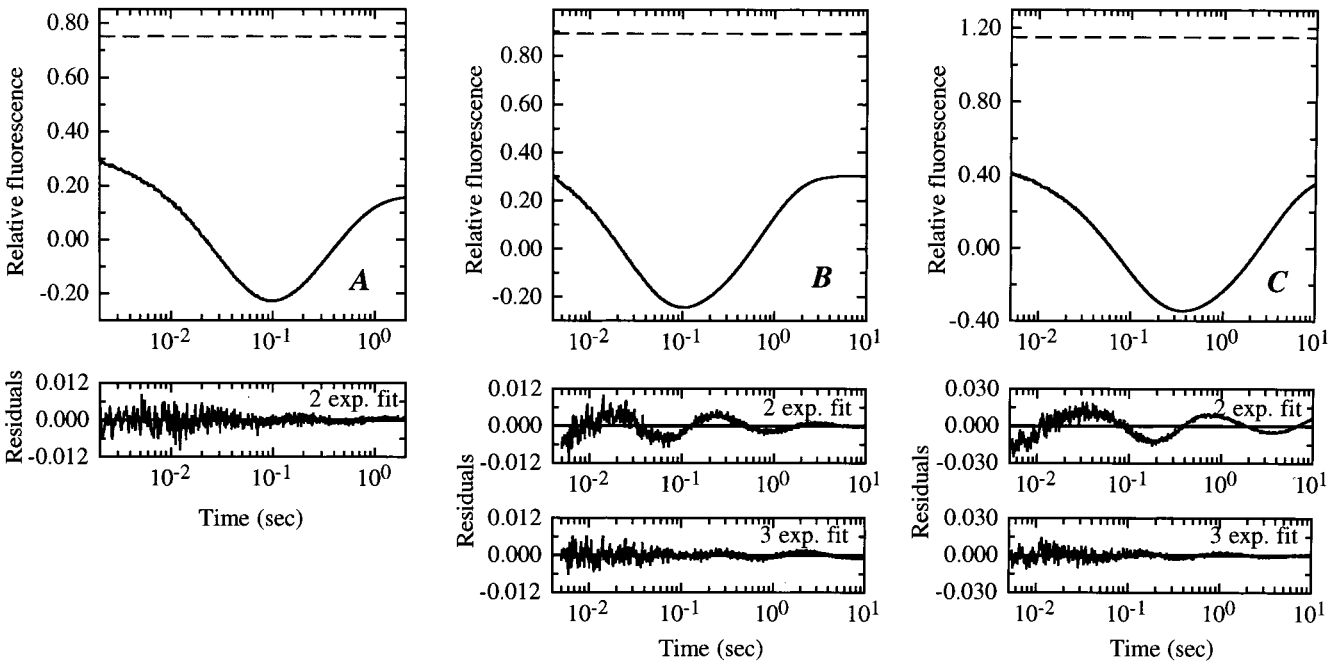

FIGURE 1: Refolding of lysozyme in the absence (a) and presence (b) of 0.85 M NaCl at 20 °C and in the presence of 0.85 M NaCl at 10 °C (c). The folding reaction was monitored by the change in intrinsic tryptophan fluorescence. Refolding conditions were 0.6 M GdmCl, 20 mM NaOAc, pH 5.2 and 20 °C. Folding in the absence of NaCl can be fit with a double exponential function with rate constants (k_{app}) of 30 ± 1 s^{-1} and 2.6 ± 0.1 s^{-1} and amplitudes of 0.70 ± 0.01 and −0.52 ± 0.01. Folding in the presence of 0.85 M NaCl at 20 °C is best described by a triple exponential function with apparent rate constants of 63 ± 5 s^{-1}, 30 ± 3 s^{-1}, and 1.35 ± 0.05 s^{-1} and amplitudes of 0.19 ±0.03, 0.53 ± 0.03, and −0.63 ± 0.01, respectively. The fit to the folding reaction in the presence of 0.85 M NaCl at 10 °C gives time constants of 33 ± 3 s^{-1}, 9.1 ± 0.3 s^{-1}, and 0.32 ± 0.02 s^{-1} (A_1 = 0.18 ± 0.02; A_2 = 0.73 ± 0.02; A_3 = −0.83 ± 0.01) The dashed line in all panels indicates the fluorescence of the unfolded protein extrapolated to refolding conditions. Under both conditions major fluorescence changes occur within the dead-time of mixing (2 ms).

± 10 ms (Figure 1A). Figure 1B displays the effect of the addition of 0.85 M NaCl on the refolding kinetics. Comparison of the residuals of double and triple exponential fits shows clearly that a third exponential is needed to fit the data in the presence of NaCl. The three observable kinetic phases have time constants of 16 ± 4 ms, 34 ± 3 ms, and 740 ± 20 ms. As in the absence of NaCl, a major part of the fluorescence is quenched in the dead-time of stopped-flow mixing (Figure 1), which can be attributed to a very rapid compaction of the polypeptide chain (*20*). Measuring the NaCl-dependence of the refolding kinetics shows that the additional faster rate constant is observed at NaCl concentrations above 100 mM and that the rate of the slowest reaction decreases steadily with increasing salt concentrations (data not shown). The presence of a third kinetic phase in the presence of NaCl is even more pronounced at 10 °C where the two faster rate constants show time constants of 30 ± 3 ms and of 110 ± 5 ms and the slower reaction has a time constant of 3.0 ± 0.1 s (Figure 1C).

To see whether the effect of NaCl is due to a general stabilizing effect of the salt, we investigated its influence on the stability of native lysozyme. Figure 2A compares equilibrium unfolding transitions of lysozyme at pH 5.2 in the presence and absence of 0.85 M NaCl. The stability ($\Delta G°$) was obtained by fitting the data to a two-state model. This resulted in $\Delta G°$ values of −46.4 ± 1.5 kJ/mol and of −49.5 ± 2.0 kJ/mol in the absence and presence of 0.85 M NaCl, respectively, which shows that NaCl has only a minor effect on lysozyme stability. This result is supported by urea-induced unfolding transitions at pH 5.2 that exhibit a similar change in $\Delta G°$ (data not shown).

To further characterize the effect of NaCl on lysozyme folding, we measured unfolding and refolding kinetics at 20 °C in the presence of 0.85 M NaCl at various concentrations of GdmCl between 0.12 and 6.3 M (Figure 2B). In addition to refolding experiments starting from the unfolded state and unfolding kinetics starting from the native protein, we measured kinetics using a double mixing procedure. In these experiments, the protein is allowed to refold for a short time in the presence of 0.6 M GdmCl to allow any partially folded intermediates to populate. After 100 ms of refolding, the reaction is interrupted by transferring the solution to higher concentrations of GdmCl (between 1.3 and 5.2 M GdmCl) and the resulting kinetics are monitored. This procedure allows the determination of the two faster rate constants (λ_2 and λ_3) over a broad range of GdmCl concentrations, which is not possible in single mixing experiments (*22*). Figure 2B shows that three apparent rate constants are needed to fit the refolding and unfolding kinetics over the complete range of GdmCl concentrations, confirming the existence of an additional kinetic phase induced by NaCl. The values and the GdmCl-dependencies of λ_2 and λ_3 are similar, whereas the slowest apparent rate constant (λ_1) is much smaller and exhibits a minimum at the midpoint of the unfolding transitions at 4.2 M GdmCl.

Time Course of Formation of Native Molecules. The results from fluorescence-detected refolding and unfolding kinetics show three apparent rate constants above 100 mM NaCl, which indicates a four-state model for lysozyme folding (*30*). Consequently, a second intermediate (I_2) is required to describe refolding under these conditions. The appearance of a new intermediate rises the question of its

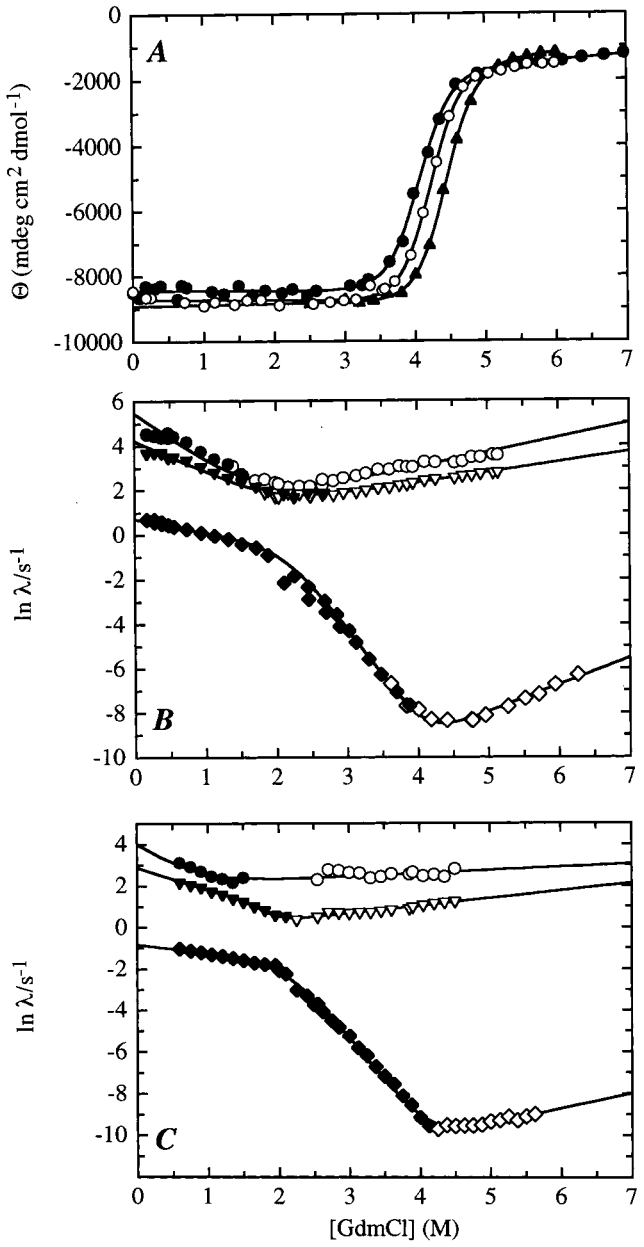

FIGURE 2: (A) Effect of NaCl on the stability of native lysozyme. The GdmCl-induced unfolding transitions were fit assuming the two-state model (*52*). This resulted in $\Delta G°$ values of -46.4 ± 1.5 kJ/mol; ($m = d\Delta G°/d$[GdmCl] $= 11.0 \pm 0.6$ (kJ/mol)/M)) and of -49.5 ± 2.0 kJ/mol, ($m = 11.7 \pm 0.7$ (kJ/mol)/M)) at 20 °C in the absence (○) and presence (●) of 0.85 M NaCl, respectively. The transition at 10 °C in the presence of 0.85 M NaCl (▲) gave values of -51.5 ± 1.9 kJ/mol ($m = 11.6 \pm 0.5$(kJ/mol)/M)). Panels (B) and (C) show the effect of GdmCl of the three apparent rate constants (λ_i) for lysozyme folding in the presence of 0.85 M GdmCl at 20 °C and at 10 °C, respectively. The data from single mixing stopped-flow refolding experiments (♦, ▼, ●) were combined with double mixing experiments. In these experiments, partially folded states were first allowed to populate for 100 ms at 0.6 M GdmCl. In a second mixing step, the intermediates were unfolded at various concentrations of denaturant in the presence of 0.85 M GdmCl. This allowed the measurement of λ_2 (▽) and λ_3 (○) over a broad range of GdmCl concentrations. The slowest folding reactions (λ_1; ◊) was measured by manual mixing unfolding and refolding experiments above 2 M GdmCl. All experiments were carried out at pH 5.2, and 20 mM NaOAc.

location on the folding pathway. The single intermediate (I_1) detected in lysozyme folding in the absence of NaCl was shown to be located on an alternative slow folding pathway. The major evidence for this came from the time course of formation of native molecules, which showed a slow folding pathway going through the helical intermediate (I_1) and an additional direct fast folding pathway (*21*). To investigate the role of the NaCl-induced intermediate (I_2), we monitored the time course of formation of native lysozyme in the presence of 0.85 M NaCl (Figure 3) using essentially the same interrupted refolding experiments that were used to detect the direct refolding pathway in the absence of NaCl (*21*). These experiments make use of the high-energy barrier between the native state and any unfolded or partially folded states (*31*, *32*). Consequently, under strongly destabilizing conditions (e.g., at high concentrations of denaturant) native molecules unfold much slower than any partially folded states and the amplitude of this slow unfolding reaction is a measure of the amount of native molecules. Starting from a completely unfolded protein, we initiated refolding by a first mixing step into 0.85 M NaCl, 0.6 M GdmCl, 20 mM NaOAc at pH 5.2 and allowed refolding to proceed for a certain time t_i. At t_i, a second mixing step was applied, which changes the solvent to 6.7 M GdmCl, pH 1.5. Under these conditions, native lysozyme unfolds with a relaxation time of 8 s. Any partially folded states unfold within 100 ms. The amplitude of the slow unfolding reaction induced after different lengths of refolding pulses (t_i) can be used as a measure for the amount of native molecules present at t_i. The resulting time course of formation of native molecules (Figure 3, A and B) indicates that native lysozyme is formed in at least two kinetic reactions in the presence of NaCl with time constants ($1/\lambda_i$) of 60 ± 30 ms and 700 ± 20 ms and amplitudes of 10 ± 2 and of 90 ± 2%, respectively. The rate of the slow unfolding reaction was essentially independent of the refolding time (t_i) and corresponds to the known unfolding rate of native lysozyme (Figure 3C). This rules out that the interrupted refolding experiments detect any transiently populated kinetic species, which might be only slightly less stable than the native state.

To test whether the time course of formation of native lysozyme is compatible with an intermediate located on the fast pathway, we simulated the fast formation of native lysozyme as a consecutive reaction. We assumed the formation of an intermediate with the rate constant λ_3 and its subsequent interconversion to the native state with λ_2. The simulations show that this mechanism produces an initial lag in formation of native lysozyme (Figure 3B). It can, however, describe formation of the native state at time points above 80 ms assuming that 11% of the molecules fold through the fast pathway. However, the early time region of formation of the native state is not very well-described by the simulations. To confirm these results with an improved resolution of the faster reactions, we monitored formation of native lysozyme at 10 °C, where folding still follows a triple exponential process but with considerably slower rates (Figure 1C). The stability of the lysozyme increases by 3.1 ± 3.9 kJ/mol by decreasing the temperature from 20 °C to 10 °C (Figure 2A). At 10 °C, formation of native lysozyme again clearly occurs in two reactions (Figure 4), and 10 ± 1% of the molecules fold through the faster pathway with a time constant of 108 ± 20 ms, which corresponds to $1/\lambda_2$ under these conditions ($1/\lambda_2 = 110 \pm 5$ ms; Figure 1C). The remaining molecules fold with a time constant of 2.8 ± 0.1 s, which corresponds to $1/\lambda_1$. As for refolding at 20 °C, a

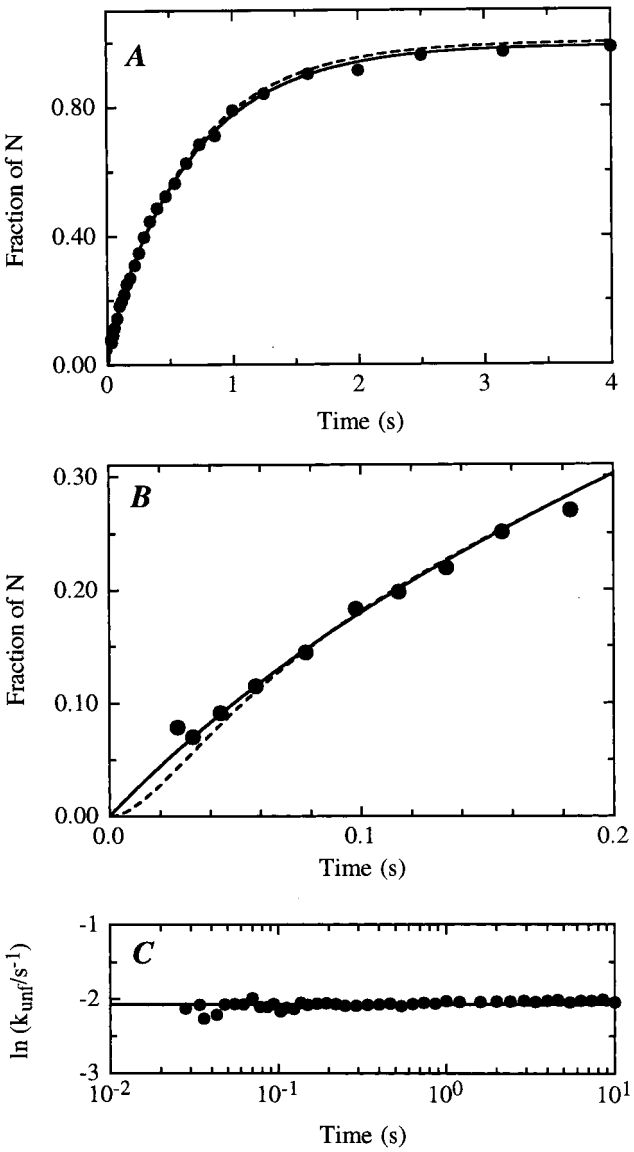

FIGURE 3: Time course of formation of native lysozyme measured by interrupted refolding experiments. Lysozyme was refolded in 0.6 M GdmCl, 0.85 M NaCl, 20 mM NaOAc at 20 °C. After various times (t_i), refolding was interrupted and the protein transferred to unfolding conditions of 6.7 M GdmCl, 50 mM Gly/HCl, pH 1.5, where native lysozyme unfolds with a time constant of 8 s. The amplitude of this unfolding reaction (●) is plotted against t_i. The solid line shows a double exponential fit of the data with time constants of 60 ± 30 ms (10 ± 2% amplitude) and of 680 ± 20 ms (90 ± 2% amplitude). A single exponential fit could not describe the data. Panel B shows the early time region of the kinetics. The dashed line represents a simulated time course of formation of N assuming two parallel pathways with an intermediate located on each pathway (Scheme 2, model 1). The intermediate on the fast pathway was assumed to form with $1/\lambda_3 = 17$ ms and decay with $1/\lambda_2 = 36$ ms and the intermediate on the slow pathway was assumed to form with $1/\lambda_2 = 36$ ms and decay with $1/\lambda_1 = 680$ ms. These rate constants were taken from the fluorescence detected refolding curves (Figures 1B and 2B). The curve was simulated by assuming that 11% of the molecules fold through the fast pathway, which gave the best reproduction of the data. Panel C show that the rate of the observed unfolding reaction (●) is independent of t_i confirming that the same state is monitored at all times t_i.

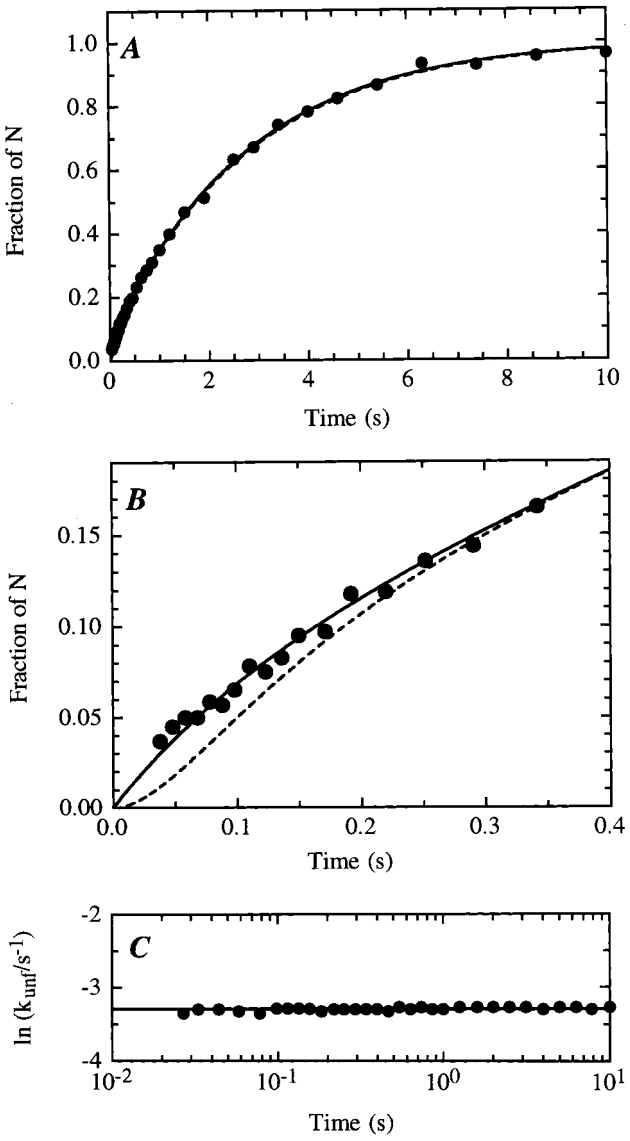

FIGURE 4: Time course of formation of native lysozyme (●) measured by interrupted refolding experiments. Lysozyme was refolded in 0.6 M GdmCl, 0.85 M NaCl, 20 mM NaOAc at 10 °C The experiments were carried out in essentially the same way as in Figure 3. A double exponential fit gave time constants of 108 ± 20 ms (10 ± 1% amplitude) and of 2.8 ± 0.1 s (90 ± 1% amplitude). A single exponential fit could not describe the data. Panel B shows the early time region of the kinetics. The dashed line represents the time course of formation of N assuming two parallel pathways with an intermediate located on each pathway (Scheme 2, model 1) and the time constants measured in direct refolding experiments (Figure 2C). The intermediate on the fast pathway was assumed to form with $1/\lambda_3 = 23$ ms and decay with $1/\lambda_2 = 110$ ms and the intermediate on the slow pathway was assumed to form with $1/\lambda_2 = 110$ ms and decay with $1/\lambda_1 = 2.8$ s. Assuming that 10% of the molecules fold through the fast pathway gave the best reproduction of the data (- - -). As for 20 °C, the rates of the observed unfolding reactions were independent of t_i (panel C).

simulation of formation of native lysozyme via an intermediate, which is formed with the fastest observable rate constant (λ_3), shows a lag corresponding to λ_3 and can clearly not reproduce the data at early time points (Figure 4B). Because of the decreased rate constants this effect is much more pronounced at 10 °C as compared to 20 °C. These results show that the fast direct folding pathway still exists in the presence of 0.85 M NaCl and that neither intermediate is located on the direct folding pathway.

Time Course of Formation of Intermediates. A high-energy intermediate had been shown to be located between collapsed lysozyme and the helical intermediate (I_1) at low-ionic

strength (*23*), which might correspond to the NaCl-induced state (I_2). In this case, formation of the helical intermediate would occur via I_2. To test for this mechanism, we monitored the time course of formation and decay of the two folding intermediates, using interrupted refolding experiments similar to those described above. This time the second mixing step produced mildly denaturing conditions (5.0 M GdmCl, 0.85 M NaCl, 20 mM NaOAc, pH 5.2, 20 °C or 10 °C) that allows the measurement of two unfolding reactions with relaxation times of 25 ms ($1/\lambda_3$) and 65 ms ($1/\lambda_2$) at 20 °C (see Figure 2B) or of 50 ms ($1/\lambda_3$) and 200 ms ($1/\lambda_2$) at 10 °C (see Figure 2C). A third reaction, corresponding to unfolding of native lysozyme was observed in the range of several thousands of seconds. This reaction did not interfere with the experiments that were carried out on the time scale between 2 ms and 1 s. At the chosen unfolding conditions only little kinetic coupling between the different pathways occurs, since all refolding steps are slow (see Figure 2, B and C). Thus, the three observable kinetic reactions correspond to the unfolding reactions of the three different folded species, namely, the native state (λ_1) and the two folding intermediates (λ_2 and λ_3, ref *23*), which was confirmed by a simulation of the interrupted refolding experiments for all possible four-state models (see Discussion). The amplitudes of the two faster unfolding reactions are thus a measure for the relative amount of the two intermediates at the time, when refolding was interrupted. Figures 5 and 6 show the time course of formation and decay of the two intermediates at 20 °C and at 10 °C, respectively. They are formed with different rates, which correspond exactly to the two faster rate constants (λ_2 and λ_3) observed in fluorescence measurements. The decay of both intermediates occurs with the slowest observable rate constant (λ_1). The populations of both states extrapolates to zero at $t = 0$, arguing for the absence of a lag phase in their formation and indicating that they are not located on a sequential pathway. This is confirmed by simulating the time course of the intermediates, assuming a sequential folding mechanism. Placing either state as the first intermediate on a sequential folding pathway cannot reproduce the experimental data (Figures 5 and 6). These results suggest that the two intermediates are located on parallel folding pathways. In addition, the experiments support the existence of a fast direct pathway by showing that none of the intermediates decays with a rate corresponding to the fast formation of native molecules (cf. Figures 3 and 4). At all time points, the unfolding kinetics could be fit by the sum of two exponentials both at 20 °C and at 10 °C corresponding to the unfolding of I_1 and I_2 and no additional slower unfolding reaction, besides unfolding of the native protein on the several thousands of seconds time scale could be detected. This rules out the presence of any additional rapidly formed intermediate.

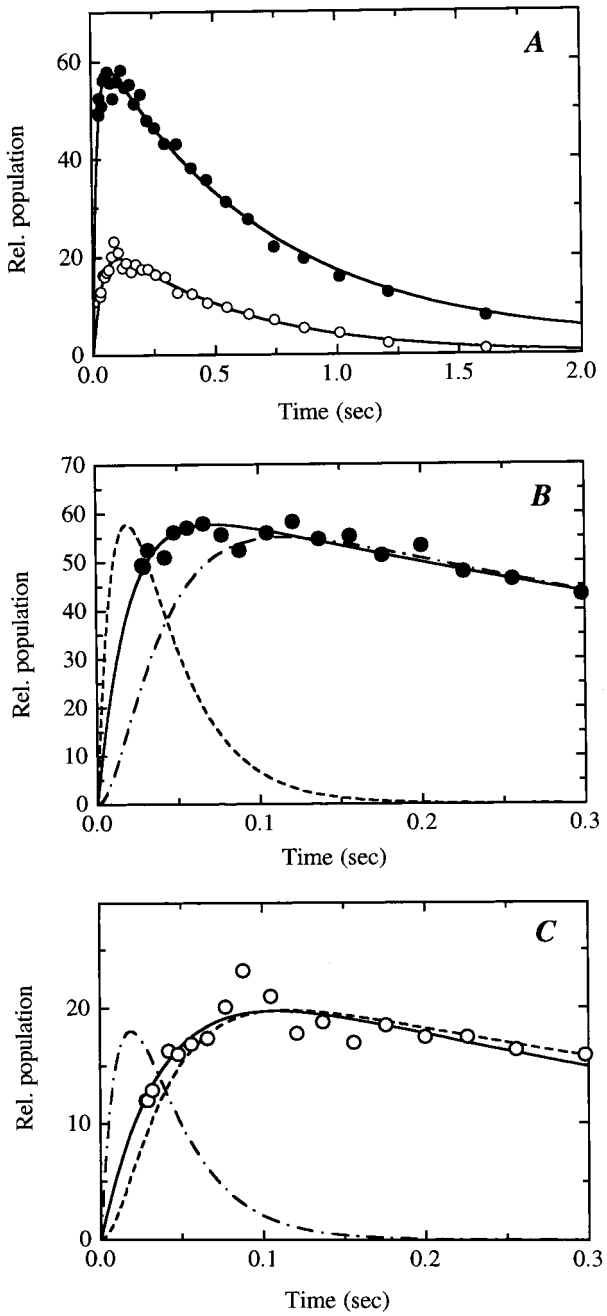

FIGURE 5: Time course of the two folding intermediates measured by interrupted refolding experiments at 20 °C. (A) complete refolding reaction (B) early time region. Refolding was carried out at 0.6 M GdmCl, 0.85 M NaCl, 20 mM NaOAc, pH 5.2. After various times t_i refolding was interrupted and unfolding of the two intermediates was monitored at 5.0 M GdmCl, 0.85 M NaCl, 20 mM NaOAc, pH 5.2. The amplitudes of the observed unfolding reactions (●, ○) are plotted as a function of t_i. Double exponential fits (solid lines) gave the following rate constants for the formation and decay of the two intermediates: 53 ± 10 s^{-1} and 1.32 ± 0.10 s^{-1} for I_1 (●) and 27 ± 5 s^{-1} and 1.82 ± 0.15 s^{-1} for I_2 (○). In all cases, the fits extrapolated to $f(I_x) = 0$ at $t = 0$. The dashed lines represent simulated curves for the time course of each intermediate, assuming that either I_1 (- - -) or I_2 (−•−•−•−) represents the first intermediate on a linear pathway with two consecutive intermediates ($U \rightarrow I_x \rightarrow I_y \rightarrow N$; Scheme 2, model 3)). The three rate constants for the kinetic reactions were taken from the direct refolding experiments (Figure 2B). In both cases, the simulated sequential folding mechanism could not describe the experimental data.

DISCUSSION

Effect of NaCl on Lysozyme Folding and Stability. We investigated the effect of NaCl on lysozyme folding. NaCl increases the stability of native lysozyme only slightly (Figure 2A). In the presence of 0.85 M NaCl, the midpoint of the GdmCl-induced unfolding transition is shifted by 0.1 M and the extrapolated stabilities at zero denaturant in the presence and absence of NaCl are similar ($\Delta\Delta G° = 3 \pm 3$ kJ/mol). This is in agreement with its position as a neutral salt in the Hofmeister series (*26*−*29*). Despite its minor effect on protein stability, NaCl changes the folding mechanism

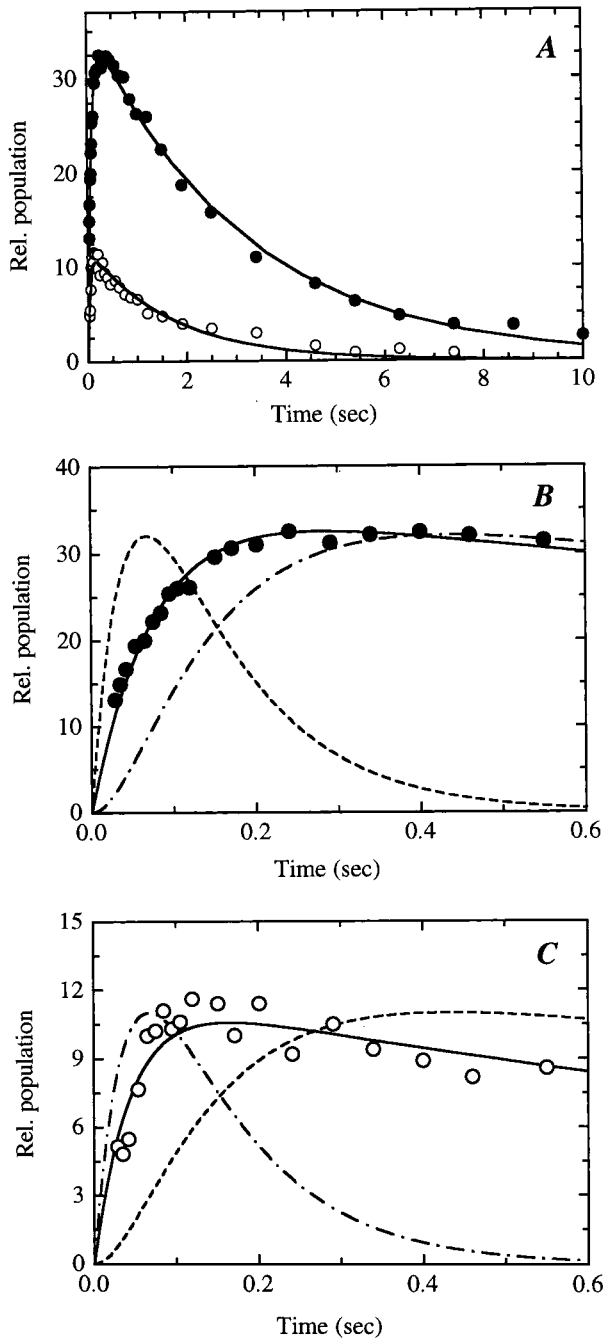

FIGURE 6: Time course of the two folding intermediates measured by interrupted refolding experiments at 10 °C. All other conditions are essentially identical as in Figure 5. Double exponential fits gave rate constants of 14 ± 2 s^{-1} and 0.32 ± 0.10 s^{-1} for I_1 (●) and of 23 ± 5 s^{-1} and 0.58 ± 0.10 s^{-1} for I_2 (○). In all cases, the fits extrapolated to $f(I_x) = 0$ at $t = 0$. The dashed lines represent the predicted time course of each intermediate, assuming that either I_1 (- - -) or I_2 (—•—•—•—) represents the first intermediate on a linear pathway with two consecutive intermediates ($U \rightarrow I_x \rightarrow I_y \rightarrow N$; Scheme 2, model 3). The three rate constants for the kinetic reactions were taken from the direct refolding experiments (Figure 2C). As in Figure 5, the sequential folding mechanism was not able to describe the experimental data.

of lysozyme. At low concentrations of NaCl (<100 mM), lysozyme exhibits double exponential folding kinetics with additional major fluorescence changes occurring in the dead-time of stopped-flow mixing (Figure 1A). This complex refolding behavior is due to rapid collapse of the polypeptide chain (*20*) followed by refolding on two parallel pathways ((*21*, *22*); Scheme 1). One of the refolding pathways leads directly to native lysozyme (*21*), whereas an intermediate with a native-like α-domain (I_1) is located on the second pathway (*19*). The coupling between the six microscopic rate constants, connecting collapsed lysozyme (C) with the intermediate (I) and the native state (N), gives rise to the two observable rate constants (*22*). The experimental observation of only two apparent rate constants despite the contribution of three microscopic equilibria is in agreement with the analytical solutions of a triangular kinetic model and holds true for any kinetic model involving three species (*30*). Collapse occurs for all molecules on a much faster time scale and can thus be treated independently in the form of a rapid preequilibrium (*33*, *34*).

Above 100 mM NaCl, a third exponential is observed during lysozyme refolding (Figure 1, B and C), indicating the presence of an additional intermediate (*35*, *36*). Under these conditions major changes in fluorescence still occur in the dead-time of stopped-flow mixing (Figure 1, B and C), showing that the additional reaction does not correspond to molecular collapse at low-ionic strength. Since protein stability is only little effected by NaCl, the stabilizing effect on the intermediate is most likely due to screening of charges in partially folded lysozyme. The ability of anions to stabilize partially folded states has been observed for many proteins under equilibrium conditions, especially at low pH (*37*, *38*) and has been attributed to the reduction of the positive net charges (*39*). For most proteins, this effect becomes only significant at low pH, when aspartate and glutamate residues titrate, resulting in a significant positive net charge on the protein. Lysozyme is a very basic protein with an isoelectric point (pI) at pH 11 and a net charge of about +12 at pH 5.2 (*40*, *41*). Consequently, the ability of chloride to screen positive charges and thus to stabilize partially folded states is already significant above the p*K* value of the acidic side chains. The presence of chloride ions from the residual amounts of GdmCl does not seem not to be sufficient to induce this effect, possibly due to a compensation by the destabilizing effect of the guanidinium ion. The intermediate can also be induced at NaCl concentrations above 50 mM when refolding is carried out in the presence of residual amounts of urea and above 30 mM NaOAc, showing that the effect does not depend on the ionic character of the denaturant or on the anion (data not shown). The induction of an additional kinetic intermediate at high ionic strength was also reported by Kulkarni et al. (*24*) on the basis of differences in the folding rates measured by hydrogen exchange and by fluorescence measurements in the presence of a variety of different salts. In these studies, only two apparent rate constants were reported in the fluorescence-detected kinetics at high-ionic strength, which would argue against the presence of an additional intermediate, unless no fluorescence change is associated with the formation of this state. Our results support the induction of an additional kinetic intermediate at high-ionic strength by showing that the expected additional rate constant can be observed.

Model for Lysozyme Folding in the Presence of NaCl. The observation of an additional folding intermediate (I_2) at high-ionic strength raises the question of its role in lysozyme folding. The time course of formation of native lysozyme in the presence of 0.85 M NaCl suggests that neither of the two intermediates is located on the direct folding pathway.

Scheme 2

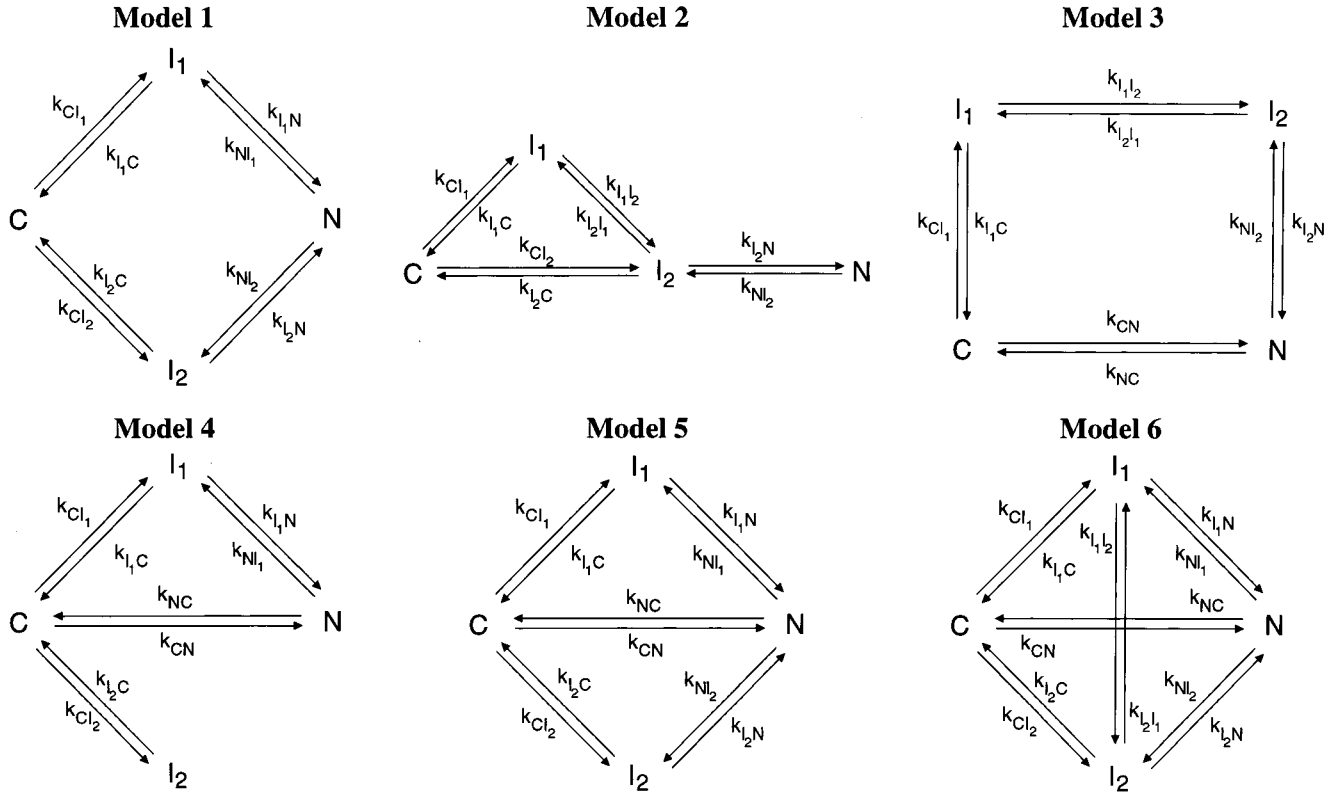

No lag phase is observed in formation of native lysozyme, indicating that a fast folding pathway still exists (Figures 3 and 5). In addition, formation of neither intermediate exhibits a lag (Figure 6), suggesting that I_1 and I_2 are not located on the same consecutive folding pathway. Both intermediates decay with the slowest observable rate constants (λ_1), which supports the data from the time course of formation of native molecules by showing that neither intermediate is located on the fast folding channel. The intermediates are formed with different rate constants both at 20 °C and at 10 °C and the rate constants are identical with the two faster rate constants from fluorescence measurements. This suggests that the system can be completely described with three apparent rate constants.

To corroborate these results and to elucidate the folding mechanism in the presence of NaCl, we fitted the time course of the different species both at 20 °C and at 10 °C to the various four-state models displayed in Scheme 2. We assumed that one of the intermediates at high-ionic strength corresponds to the previously characterized helical intermediate at low-ionic strength (I_1), since NaCl is not expected to destabilize I_1. We, thus, did not consider any models that are not in agreement with our earlier observations that I_1 is located on a parallel but direct folding pathway (*22*). Fitting the data to models 1−6 shows that only models 4, 5, and 6 can give satisfactory fits. All other models predict a lag in either the formation of native molecules (model 1), in formation of one of the intermediates (model 3) or on both pathways (model 2), which is in agreement with the simulations shown in Figures 3−6. As expected, also the three-state mechanism for lysozyme folding at low-ionic strength (Scheme 1) was not able to describe the data. Treating rapid collapse as a preequilibrium in any of the models did not change these results. To distinguish which of the three remaining models (models 4, 5, and 6) describes lysozyme folding above 100 mM NaCl, we compared the fitted microscopic rate constants with the values expected from the GdmCl-dependence of the refolding and unfolding reactions (Figure 2, B and C). As discussed above, the two fastest observable rate constants (λ_2 and λ_3) correspond to unfolding rates of the two intermediates at high concentrations of denaturant, when the unfolding rates are much higher than the refolding rates. Thus, we can extrapolate the values of λ_2 and λ_3 from the linear region above 3 M GdmCl in Figures 2B and 4B to the refolding conditions of 0.6 M GdmCl. These values can be used as estimates of the unfolding rate constants of the intermediates (k_{I_1U} and k_{I_2U}) under the conditions of the refolding experiments. Both at 10 and 20 °C, the results of fits to model 6 give values k_{I_1U} and k_{I_2U}, which are in excellent agreement with those expected for the extrapolation (compare Figures 4 and 7). The values obtained for models 4 and 5, in contrast, differ more than 5-fold from the expected rate constants. This suggests that the data are best described by model 6. The same results were obtained for fitting the time course of all species for refolding at 1.5 M GdmCl at 10 and 20 °C (data not shown). These results suggest that the NaCl-induced state is not a dead-end intermediate and that a pathway for interconversion between the two intermediates exists (Figure 7C). Figure 7, A and B, show that the time course of native molecules and of both intermediates are well-described by the fit to model 6. About 15% of refolding molecules remain in the rapidly formed collapsed state after the intermediates have formed and are interconverted to the native state in the final slow step. This has also been observed for folding at 20 °C at low-ionic strength (*20*) and indicates that both intermediates are only marginally more stable than collapsed lysozyme (cf. Figure 7C).

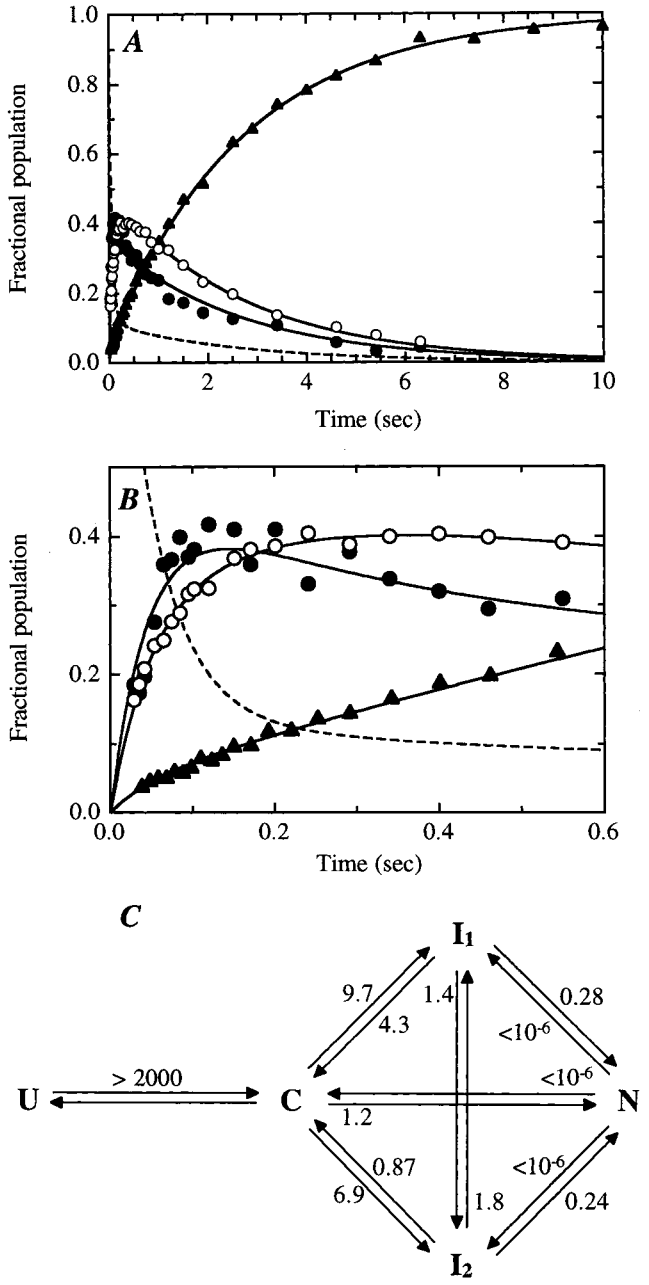

FIGURE 7: (A) Time course of the two transient intermediates I_1 (●) and I_2 (○) and of native lysozyme (▲) at 0.6 M GdmCl, 0.85 M NaCl, 20 mM NaOAc, pH 5.2 at 10 °C. (B) Early time region of the kinetics. The lines represent the results of a global fit of the three data sets to the mechanism displayed in panel C. The dashed line indicates the resulting population of collapsed lysozyme (C). Panel C shows the model that gave the best fit of the experimental data and the microscopic rate constant (k_{ij}) from the fit. The populations of I_1 and I_2 were normalized to the actual populations of the two states obtained from the fit.

In addition to the microscopic rate constants, the fit also yields spectroscopic parameters for the different species, i.e. their relative fluorescence intensities. These values are nearly identical for folding at 10 and at 20 °C and show that one of the intermediates has a largely quenched tryptophan fluorescence compared to native lysozyme. Its relative fluorescence corresponds to the value observed for I_1 in the absence of NaCl (*20*). The second intermediate, in contrast, has native-like tryptophan fluorescence. This allows the assignment of the two intermediates in the kinetic model shown in Figure 7C to I_1 and I_2. The helical intermediate (I_1) was shown to have has all tryptophan side-chains located in a solvent inaccessible (*42*) and extremely hydrophobic environment (*20*). Since the fluorescence properties of native lysozyme are mainly determined by the solvent exposed tryptophan 62 in the β-domain (*43*), the markedly different fluorescence properties of I_1 compared to native lysozyme indicate nonnative side-chain interactions between hydrophobic residues in the β-domain (*20*). This is supported by folding studies on lysozyme variants with amino acid replacements in the hydrophobic regions of the β-domain (*44*). The native-like fluorescence properties of I_2 indicate major differences in the side-chain interactions in the β-domain between I_1 and I_2. This is in agreement with results of hydrogen−deuterium exchange measurements at high ionic strength, which suggested that the salt-induced intermediate (I_2) has native-like secondary structure in the α- and β-domains (*24*), whereas I_1 was shown to have native-like secondary structure only in the α-domain (*19*). However, the native-like properties of the β-domain in I_2 do not seem to promote its folding, since both intermediates react to the native state with nearly identical rates (Figure 7).

The Energy Landscape of Lysozyme Folding. Our results show that the NaCl-induced intermediate is located on neither of the two folding pathways observed at low ionic strength. We can also rule out the presence of additional native-like intermediates, since the interrupted refolding experiments aimed at the detection of partially folded states (Figures 5 and 6) do not detect any intermediates besides I_1 and I_2. The rapid formation of a native-like intermediate would be detected by these experiments unless it unfolds within the dead-time of mixing (2 ms), which is not in agreement with a native-like structure. A native-like intermediate is also not observed in the experiments sensitive for the population of native molecules (Figures 3 and 4). A near-native stability of this state would result in an additional faster unfolding rate or would lead to deviations in the observed unfolding rate at short refolding times, when the intermediate is maximally populated. This is not observed as shown in Figures 3C and 4C. These results show that I_1 and I_2 are the only intermediates populated during refolding of lysozyme at high-ionic strength and suggest that I_2 corresponds to the native-like state detected in hydrogen−deuterium exchange experiments (*19*, *24*, *45*). Since I_2 can be induced already at low-salt concentrations (≥100 mM NaCl or ≥30 mM NaOAc) the observation of I_2 in hydrogen-exchange experiments at lower ionic strength might be attributed to higher salt concentrations used in the first refolding step and/or in the exchange pulse of the hydrogen−deuterium exchange experiments (*19*). This strong dependence of the folding mechanism on salt concentrations might thus explain the differences in the rate constants observed by hydrogen exchange and by optical probes discussed by Itzhaki et al. (*42*) and by Matagne et al. (*25*) for lysozyme folding at low-ionic strength. This is supported by a comparison of the rate constants for the formation of the native-like intermediate in pulse-labeling experiments (*45*) and for the fastest process detected by fluorescence measurements at high-salt concentrations (λ_3, Figure 1B), which differ only by a factor of 2. This is a rather good agreement considering the different salt concentrations used in the different studies and the limited-number of time points obtained in the pulse-labeling experiments (*45*, *46*). The folding studies reported by

Kulkarni et al. (*24*) proposed that I_2 is additionally formed with a time constant of 350 ms in the presence of KCl on a pathway via I_1 and that I_2 represents the merging point of the slow and the fast folding pathway. This conclusion was based on a 1.4-fold difference in the slowest kinetic reaction monitored by fluorescence and by hydrogen exchange, which seems to be within the limits of experimental error of the hydrogen−deuterium exchange experiments (*24*). Our results on lysozyme folding in the presence of NaCl monitored by fluorescence and by interrupted refolding measurements show no evidence for an additional slow time constant. The decay of I_1 occurs with the same time constant as formation of native lysozyme and formation and decay of I_1, I_2, and N can be perfectly described by the three apparent rate constants detected by fluorescence (Figure 7). Our results rule out that I_2 is an essential intermediate on both the slow and the fast pathway (Scheme 2, model 2) as suggested by Kulkarni et al. (*24*). They rather show that I_2 is located on a new parallel folding pathway (Figure 7).

The intermediate I_2 is stabilized by a reduction of the electrostatic repulsion at low concentrations of NaCl under conditions when the overall protein stability is virtually unchanged. This shows that I_2 is only marginally less stable than collapsed lysozyme at low-ionic strength and suggests that it represents a metastable high-energy state on a parallel folding pathway under these conditions. The amplitude of the fast folding pathway drops from 20% at low ionic strength (*21*) to 10% when I_2 becomes populated. This suggests that the pathway going through I_2 contributes to the fast folding pathway under conditions, when I_2 is a high-energy intermediate. The barriers between the different states populated during lysozyme folding are of similar height, allowing for transitions between all four kinetic species (Figure 7). This shows that none of the populated intermediates facilitates refolding despite the presence of preformed native-like secondary structure. These results might require a re-interpretation of our previous experiments on the mechanism of formation of I_1 (*23*). In these studies, refolding was performed at low-ionic strength and the presence of intermediates was monitored by a subsequent unfolding step at high concentrations of GdmCl, similar to the interrupted refolding experiments shown in Figures 3 and 4. Although only a single fast reaction was observed in refolding, two fast reactions were observed in the unfolding step indicating the presence of two intermediates. Since both intermediates were formed with identical rates, we concluded that the second intermediate represents a high-energy intermediate on the pathway of formation of I_1. The similar stabilities of I_1 and I_2 at high concentrations of Cl^- and the low barrier for interconversion between I_1 and I_2 might lead to a significant population of I_2 at high concentrations of GdmCl in the absence of NaCl. Consequently, the previously postulated high-energy intermediate might correspond to I_2, which is also a high-energy intermediate at low-ionic strength. Further experiments will be necessary to discriminate between these models.

High-energy intermediates have previously been detected in unfolding reactions of arc repressor (*12*), staphylococcal nuclease (*13*), and CI2 (*14*) by a nonlinearity in the denaturant dependence of the free energy of activation. However, in these cases the intermediates could not be stabilized and thus could not be observed directly. A partially folded state could be induced during refolding in a mutant of ubiquitin by addition of the strongly stabilizing sulfate anion (*47*). This state was suggested to represent an obligatory intermediate on a linear folding pathway. High-energy intermediates have also been detected by native state hydrogen exchange in several proteins (*48*, *49*) and it is a point of discussion whether these states are located on a single sequential folding pathway (*50*, *51*). Although hydrogen exchange measurements are able to determine the stability of these states relative to the native state, they are not able to tell their role in the folding process. Our results show that the energy landscape of lysozyme folding contains several high-energy intermediates, some of which are only marginally less stable than unfolded lysozyme and can thus be observed even under mildly stabilizing folding conditions. The results show clearly that none of the high-energy intermediates detected in lysozyme is located on the direct folding pathway and that a number of parallel pathways with high-energy intermediates may exist. This demonstrates that the presence of high-energy intermediates does not automatically identify them as essential intermediates on a linear folding pathway.

It seems likely that the energy landscape for lysozyme folding is even more complex and might comprise of more intermediates, which are less stable than the NaCl-induced state. The presence of an additional parallel folding pathway supports the picture of many parallel folding routes from the ensemble of unfolded molecules to the native state. Consequently, the experimentally observed rate constants contain contributions from many different parallel reactions. This might contribute to the difficulty to interpret many properties of folding reactions the like temperature-dependence of the folding rates or the ϕ-value analysis in mutational studies.

REFERENCES

1. Kim, P. S., and Baldwin, R. L. (1990) *Annu. Rev. Biochem. 59*, 631−660.
2. Bryngelson, J. D., and Wolynes, P. G. (1989) *J. Phys. Chem. 93*, 6902−6915.
3. Thirumalai, D. (1994) in *Statistical Mechanics, Protein Structure, and Protein Substrate Interactions* (Doniach, S., Ed.) pp 115−134, Plenum Press.
4. Bryngelson, J. D., Onuchic, J. N., Socci, N. D., and Wolynes, P. G. (1995) *Proteins: Struct., Funct., Genet. 21*, 167−195.
5. Jackson, S. E., and Fersht, A. R. (1991) *Biochemistry 30*, 10428−35.
6. Alexander, P., Orban, J., and Bryan, P. (1992) *Biochemistry 31*, 7243−7248.
7. Viguera, A. R., Martínez, J. C., Filimonov, V. V., Mateo, P. L., and Serrano, L. (1994) *Biochemistry 33*, 2142.
8. Villegas, V., Azuga, A., Catasús, L., Reverter, D., Mateo, P., Avilés, F., and Serrano, L. (1995) *Biochemistry 34*, 15105−15110.
9. Kragelgund, B. B., Robinson, C. V., Knudsen, J., and Dobson, C. M. (1995) *Biochemistry 34*, 7117−7224.
10. Schindler, T., Herrler, M., Marahiel, M. A., and Schmid, F. X. (1995) *Nat. Struct. Biol. 2*, 663−673.
11. Schönbrunner, N., Koller, K.-P., and Kiefhaber, T. (1997) *J. Mol. Biol. 268*, 526−538.
12. Jonsson, T., Waldburger, C. D., and Sauer, R. T. (1996) *Biochemistry 35*, 4795−4802.
13. Walkenhorst, W. F., Green, S., and Roder, H. (1997) *Biochemistry 36*, 5795−5805.
14. Oliveberg, M., Tan, Y.-J., Silow, M., and Fersht, A. R. (1998) *J. Mol. Biol. 277*, 933−943.

15. Wolynes, P. G. (1997) *Proc. Natl. Acad. Sci. U.S.A. 94*, 6170−6175.
16. Portman, J. J., Takada, S., and Wolynes, P. G. (1998) *Phys. Rev. Lett. 81*, 5237−5240.
17. Kuwajima, K., Hiraoka, Y., Ikeguchui, M., and Sugai, S. (1985) *Biochemistry 24*, 874−881.
18. Chaffotte, A. F., Guillou, Y., and Goldberg, M. E. (1992) *Biochemistry 31*, 9694−9702.
19. Radford, S. E., Dobson, C. M., and Evans, P. A. (1992) *Nature 358*, 302−307.
20. Segel, D., Bachmann, A., Hofrichter, J., Hodgson, K., Doniach, S., and Kiefhaber, T. (1999) *J. Mol. Biol. 288*, 489−500.
21. Kiefhaber, T. (1995) *Proc. Natl. Acd. Sci. U.S.A. 92*, 9029−9033.
22. Wildegger, G., and Kiefhaber, T. (1997) *J. Mol. Biol. 271*, 294−304.
23. Kiefhaber, T., Bachmann, A., Wildegger, G., and Wagner, C. (1997) *Biochemistry*, 5108−5112.
24. Kulkarni, S. K., Ashcroft, A. E., Carey, M., Masselos, D., Robinson, C. V., and Radford, S. E. (1999) *Protein Sci. 8*, 35−44.
25. Mantagne, A., Radford, S. E., and Dobson, C. M. (1997) *J. Mol. Biol. 267*, 1068−1074.
26. Lewith, S. (1888) *Arch. Exp. Pathol. Pharmakol. 24*, 1−16.
27. Hofmeister, F. (1888) *Arch. Exp. Pathol. Pharmakol. 24*, 247−260.
28. von Hippel, P. H., and Wong, K.-Y. (1965) *J. Biol. Chem. 240*, 3909−3923.
29. Baldwin, R. L. (1996) *Biophys. J. 71*, 2056−2063.
30. Matsen, F. A., and Franklin, J. L. (1950) *J. Am. Chem. Soc. 53*, 3337−3341.
31. Segawa, S., and Sugihara, M. (1984) *Biopolymers 23*, 2437−2488.
32. Schmid, F. X. (1986) *Methods Enzymol. 131*, 70−82.
33. Hill, T. L. (1974) *Prog. Biophys. Mol. Biol. 28*, 267−340.
34. Hill, T. L. (1977) *Free Energy Transduction in Biology.*, Academic Press, London.
35. Szabo, Z. G. (1969) in *Comprehensive chemical kinetics* (Bamford, C. H., and Tipper, C. F. H., Eds.) pp 1−80, Elsevier Publishing Company, Amsterdam.
36. Moore, J. W., and Pearson, R. G. (1981) *Kinetics and Mechanisms.*, John Wiley & Sons, New York.
37. Goto, Y., Calciano, L. J., and Fink, A. L. (1990) *Proc. Natl. Acad. Sci. U.S.A. 87*, 573−577.
38. Goto, Y., Takahashi, N., and Fink, A. L. (1990) *Biochemistry 29*, 3480−3488.
39. Goto, Y., and Nishikiori, S. (1991) *J. Mol. Biol. 222*, 679−686.
40. Tanford, C., and Roxby, R. (1972) *Biochemistry 11*, 2192−2198.
41. Behlke, J., and Ristau, O. (1999) *Biophys. Chem. 76*, 13−23.
42. Itzhaki, L. S., Evans, P. A., Dobson, C. M., and Radford, S. E. (1994) *Biochemistry 33*, 5212−5220.
43. Imoto, T., Forster, L. S., Rupley, J. A., and Tanaka, F. (1972) *Proc. Natl. Acad. Sci. U.S.A. 69*, 1151−1155.
44. Rothwarf, D. M., and Scheraga, H. A. (1996) *Biochemistry 35*, 13797−13807.
45. Miranker, A. D., Robinson, C. V., Radford, S. E., Aplin, R. T., and Dobson, C. M. (1993) *Science 262*, 896−900.
46. Radford, S. E., Buck, M., Topping, K. D., Dobson, C. M., and Evans, P. A. (1992) *Proteins 14*, 237−48.
47. Khorasanizadeh, S., Peters, I. D., and Roder, H. (1996) *Nat. Struct. Biol. 3*, 193−205.
48. Bai, Y., Sosnick, T. R., Mayne, L., and Englander, S. W. (1995) *Science 269*, 192−197.
49. Chamberlain, A. K., Handel, T. M., and Marqusee, S. (1996) *Nat. Struct. Biol. 3*, 782−787.
50. Clarke, J., Itzhaki, L. S., and Fersht, A. R. (1997) *Trends. Biochem. Sci. 22*, 284−287.
51. Englander, S. W. (1998) *Trends Biochem. Sci 23*.
52. Santoro, M. M., and Bolen, D. W. (1988) *Biochemistry 27*, 8063−8068.

BI9909703